Research Paper

Journal of Chemical Research

Journal of Chemical Research
1–10

DOI: 10.1177/1747519820976543
journals.sagepub.com/home/chl
SAGE

Synthesis, characterization, crystal structures, and the biological evaluation of 2-phenylthiazole derivatives as cholinesterase inhibitors

Da-Hua Shi[1,2,3], Meng-qiu Song[2], Xiao-Dong Ma[2], Jia-Bin Su[2], Jing Wang[2], Xiu-Jun Wang[2], Yu-Wei Liu[2], Wei-Wei Liu[2] and Xin-Xin Si[2]

Abstract

Four 2-phenylthiazole derivatives are synthesized, characterized, and evaluated as cholinesterase inhibitors. The structures of the 2-phenylthiazole derivatives are confirmed by ^{1}H and ^{13}C nuclear magnetic resonance spectroscopy, single-crystal X-ray diffraction studies, and Hirshfeld surfaces analysis. Hirshfeld surface analysis of the prepared compounds showed C–H···O intermolecular interactions. The cholinesterase inhibition activities of the synthesized compounds are tested by Ellman's method. [2-(4-Benzyloxyphenyl)-thiazol-4-yl]-(3,5-dimethylpiperidin-1-yl)-methanone showed the best acetylcholinesterase inhibition activity with an IC_{50} value of 8.86 μM and the best butyrylcholinesterase inhibition activity with an IC_{50} value of 1.03 μM. A docking study demonstrates that the same compound interacts with the catalytic anionic site and peripheral anionic site of acetylcholinesterase and the catalytic anionic site of butyrylcholinesterase.

Keywords

Alzheimer's disease, cholinesterase, crystal structure, 2-phenylthiazole derivatives

Date received: 17 August 2020; accepted: 6 November 2020

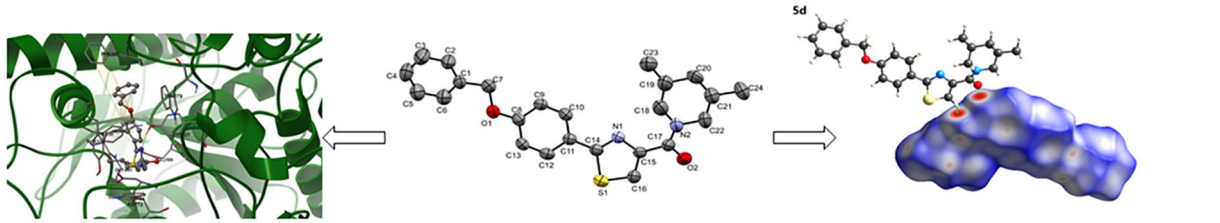

Molecular Docking of compound **6d**

Potent AChE and BuChE inhibitor (**6d**)
IC_{50} for AChE 8.86 μM
IC_{50} for BuChE 1.03 μM

Hirshfeld surface analysis of compound **6d**

Introduction

Alzheimer's disease (AD) is one of the major diseases threatening the health of the elderly in modern society. AD is a chronic progressive neurodegenerative disease that worsens over time.[1] The common early symptoms are forgetfulness and cognitive dysfunction. As the disease progresses, it can lead to serious language problems, disorientation, loss of self-management, and even gradual loss of physical functions, eventually leading to death.[2] The incidence of AD is progressively increasing across the world due to an aging population.[3] Therefore, it is of great significance to develop effective anti-AD drugs.

Five drugs are currently used to treat AD cognitive dysfunction, four of which are acetylcholinesterase inhibitors

[1]Jiangsu Key Laboratory of Marine Biotechnology, Jiangsu ocean university/Jiangsu Key Laboratory of Marine Bioresources and environment, Jiangsu ocean university, Lianyungang, P.R. China
[2]School of Pharmacy, Jiangsu Ocean University, Lianyungang, P.R. China
[3]Co-Innovation Center of Jiangsu Marine Bio-Industry Technology, Lianyungang, P.R. China

Corresponding authors:
Da-Hua Shi, School of Pharmacy, Jiangsu Ocean University, Lianyungang 222005, Jangsu, P.R. China.
Email: shidahua@jou.edu.cn

Xin-Xin Si, School of Pharmacy, Jiangsu Ocean University, Lianyungang 222005, Jangsu, P.R. China.
Email: sixx@jou.edu.cn

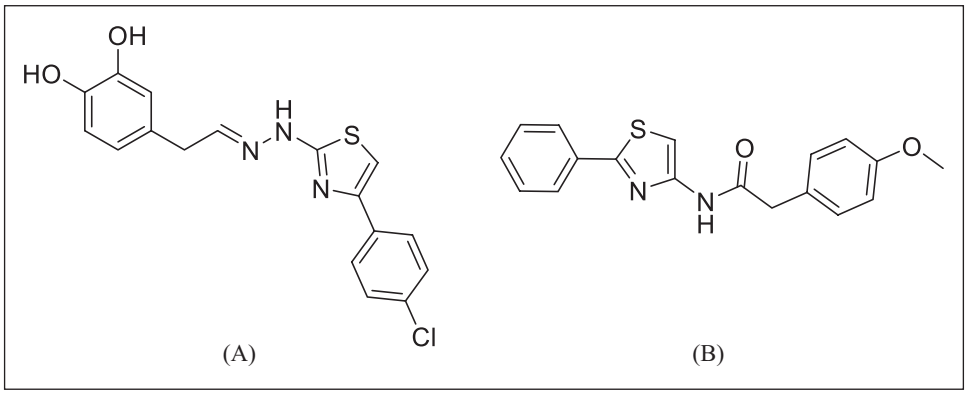

Figure 1. Chemical structures of (*E*)-4-({2-[4-(4-chlorophenyl)thiazol-2-yl]hydrazono}methyl)benzene-1,2-diol (compound **A**) and 2-(4-methoxyphenyl)-*N*-(4-phenylthiazol-2-yl)acetamide (compound **B**).

(AChEIs): tacrine,[4] donepezil,[5,6] galantamine,[7] and rivastimine.[8] Acetylcholinesterase (AChE) is considered as the main factor responsible for acetylcholine (ACh) metabolism, and AChEIs can effectively prevent the hydrolysis of ACh and provide a promising therapeutic effect.[9] In recent decades, the role of butyrylcholinesterase (BuChE) in the development of AD has been clarified. Evidence indicates that BuChE is related to some important AD hallmarks such as the extracellular deposition of the amyloid ·-protein(A·) and the aggregation of hyperphosphorylated tau protein.[10] The activity of AChE is decreased during the course of AD progression, while the activity of BuChE is stable or even increased, which is a compensatory feedback of ACh metabolism and cannot be overcome clinically at present.[11] Consequently, the simultaneous inhibition of both enzymes may be a more attractive therapeutic strategy in AD.

Thiazole containing compounds have a variety of biological activities such as antioxidant, anti-inflammatory, antitumor, antiviral, and cholinesterase inhibition activity.[12] Thiazole and its derivatives have attracted continuing interest for the design of various novel central nervous system (CNS) active agents. In the past few decades, thiazoles have been widely used to develop a variety of therapeutic agents against numerous CNS targets.[13] Many thiazole derivatives have been reported to possess cholinesterase inhibitory activities.[14–16] For instance, Rahim et al.[17] studied the potential inhibitory activity of 30 thiazole analogues against AChE and BuChE, among which (*E*)-4-({2-[4-(4-chlorophenyl)thiazol-2-yl] hydrazono}methyl)benzene-1,2-diol (compound **A**) possessed the best AChE-inhibition activity (IC_{50} = 21.3 μM) and the best BuChE-inhibition activity (IC_{50} = 1.59 μM). Sun et al.[16] reported that 2-(4-methoxyphenyl)-*N*-(4-phenylthiazol-2-yl)acetamide (compound **B**) showed the best AChE inhibitory activity with an IC_{50} value of 3.14 μM. Thiazole containing compounds can be used as lead compounds to develop new cholinesterase inhibitors (Figure 1).

Previously, several studies with thiazole-derived AChEIs have demonstrated that the thiazole ring primarily interacts with peripheral anionic site (PAS) of AChE and the amine functional moiety interacts with catalytic anionic site (CAS) of AChE.[18,19] To find novel dual binding site inhibitors of AChE, we attempted to connect the 2-phenylthiazole moiety (binding to PAS) with amine functional moieties (binding to CAS) to design a series of new 2-phenylthiazole derivatives as dual binding site inhibitors of AChE (Figure 2).

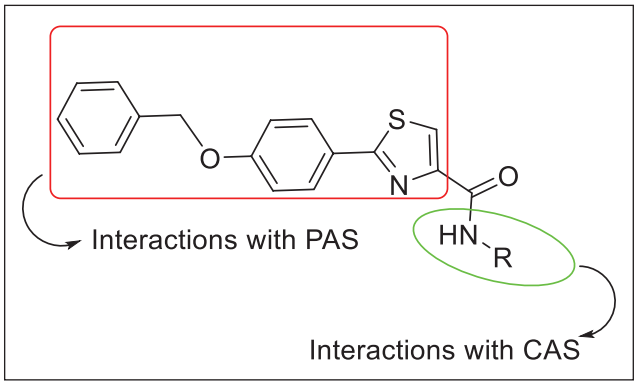

Figure 2. Design strategy of the target compounds.

In this study, four novel 2-phenylthiazole derivatives have been synthesized and characterized. The intermolecular interactions of these compounds were analyzed through single-crystal X-ray structure studies and Hirshfeld surface analysis. Furthermore, these derivatives were subjected to biological evaluation as potential inhibitors of AChE and BuChE. Finally, molecular docking studies of the most potent inhibitors were carried out to determine the binding interactions with AChE and BuChE, respectively.

Results and discussion

Spectral characterization

The synthetic route to compounds **6a–d** is presented in Scheme 1. Condensation of 4-hydroxythiobenzamide (**1**) and ethyl bromopyruvate (**2**) in refluxing EtOH for 4 h gave ethyl 2-(4-hydroxyphenyl)thiazole-4-carboxylate (**3**). Compound **3** was *O*-alkylated by treatment with benzyl[20] bromide in dimethylformamide (DMF) at 80 °C to afford compound **4**. The desired products were synthesized via saponification, acyl chlorination, and acylamination with compound **4** as the starting material. Crude products **6a–d** were purified by silica gel column chromatography. The purities of the obtained compounds were checked by thin-layer chromatography (TLC). The compounds were characterized by Fourier-transform infrared spectroscopy (FTIR), ^{1}H nuclear magnetic resonance (NMR), ^{13}C NMR, and X-ray crystallography. All the results substantiate the structures proposed.

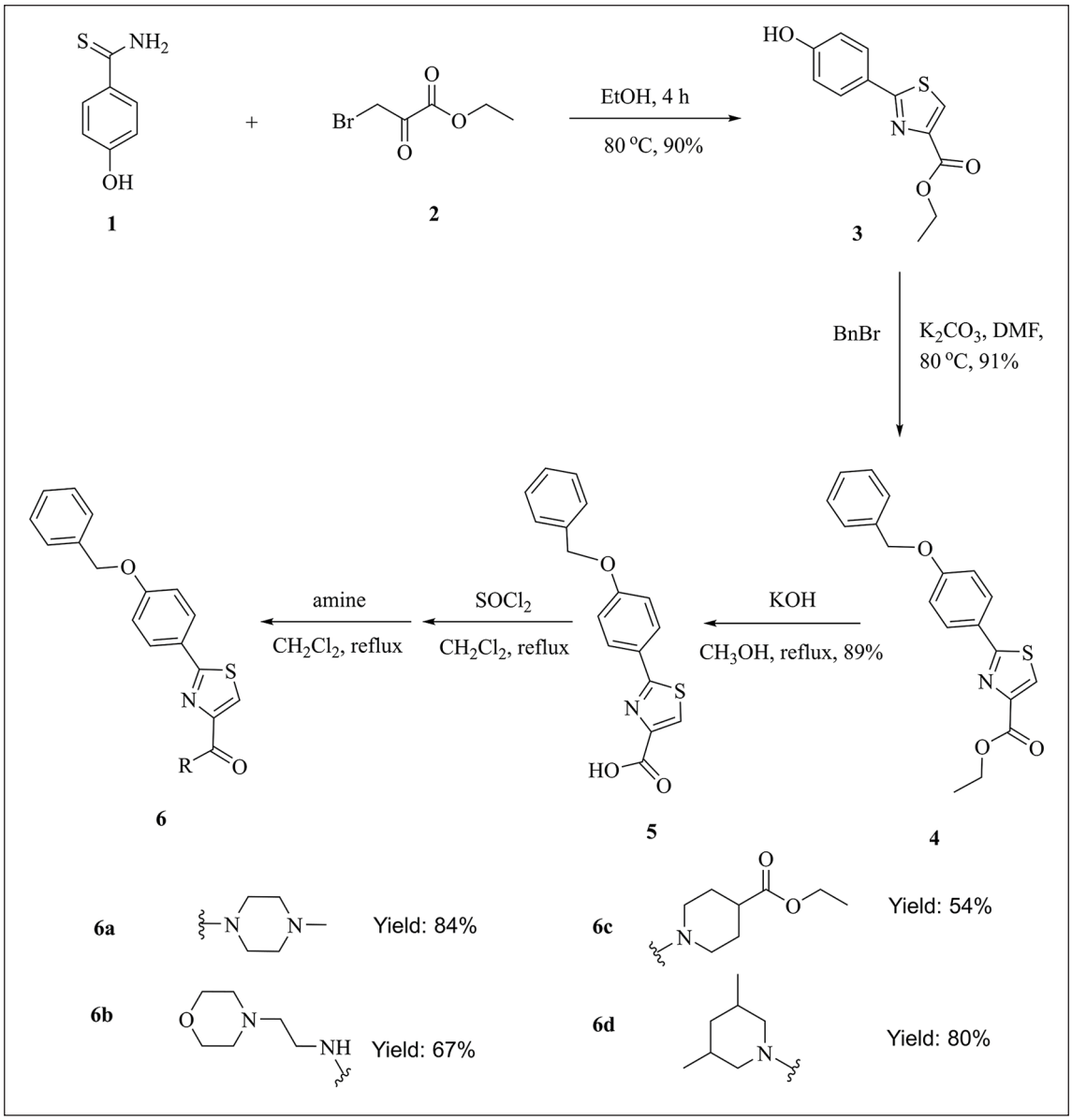

Scheme 1. Synthesis of 2-phenylthiazole derivatives **6a–d.**

The FTIR spectra of the prepared compounds are characterized by a strong broad absorption in the range of 1603–1629 cm^{-1}, which can be assigned to the υ (C=O) stretches. The absorption bands falling in the range of 2810–2971 cm^{-1} correspond to υ (C–H) of the alkane chain in compounds **6a–d**. The υ (C–H) mode appears in the range of 3079–3088 cm^{-1}, suggesting the presence of aromatic benzene rings in the four products. The ^{1}H NMR spectra of the prepared compounds displayed protons due to a thiazole ring at 7.83, 8.01, 7.80, and 7.75 ppm, respectively, as singlets. The protons of 1,4-disubstituted benzene ring were observed as two 2 H doublets at 7.88, 7.89, 7.88, and 7.88 ppm, respectively, for compound **6a–d**. The remaining signals of the protons of compounds **6a–d** were found to be in their expected region(s). In the ^{13}C NMR spectra, the characteristic phenyl signals were observed at 115.3–160.7 ppm for compounds **6a–d**. The signals of the carbonyl groups were observed at 162.7, 161.2, 162.9, and 162.6 ppm for compounds **6a–d**, respectively. The high-resolution mass spectroscopy (HRMS) spectra of compounds **6a–d** show $[M + H]^+$ peaks at *m/z*: 394.1620, 424.1727, 451.1726, and 407.1827 corresponding to $C_{22}H_{24}N_3O_2S$ $[M + H]^+$, $C_{23}H_{26}N_3O_3S$ $[M + H]^+$, $C_{25}H_{27}N_2O_4S$ $[M + H]^+$, and $C_{24}H_{28}N_2O_2S$ $[M + H]^+$.

Crystal structure of compounds **6a** *and* **6d**

The structures of compounds **6a** and **6d** were confirmed by X-ray diffraction analysis. The crystal data are presented in Table 1 in the ESI and Figures 3–6. Compound **6a** had a monoclinic crystal system and a $P2_1/n$ space group. Compound **6d** was triclinic with a P-1 space group. The selected bond lengths and angles of compounds **6a** and **6d** are listed in Table 2 in the Supplemental material. Compounds **6a** and **6d** possessed similar bond lengths with S1–C14 (1.737 and 1.724 Å), S1–C16 (1.701 and 1.681 Å), and N1–C14 (1.310 and 1.300 Å). The O1–C8 bond lengths for compounds **6a** and **6d** were 1.364 and 1.362 Å, respectively. The bond lengths of N2–C17 for compounds **6a** and

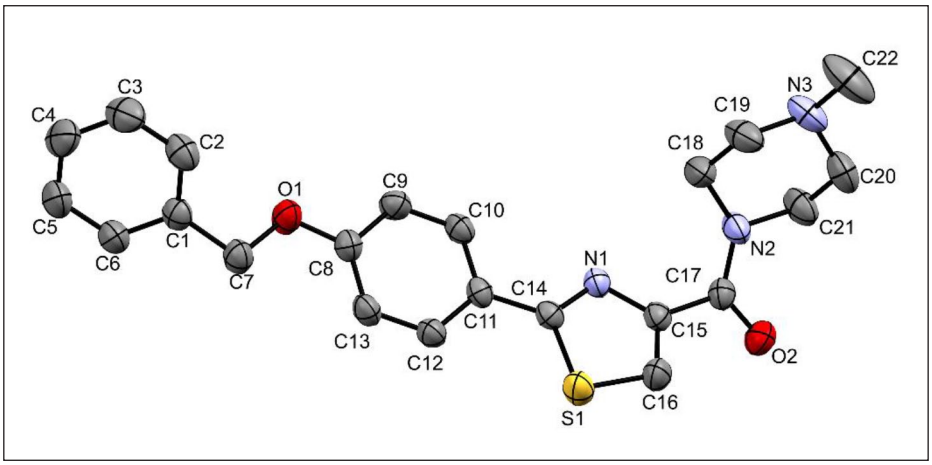

Figure 3. Oak Ridge Thermal Ellipsoid Plot (ORTEP) representation of compound **6a** with thermal ellipsoids drawn at 50% probability.

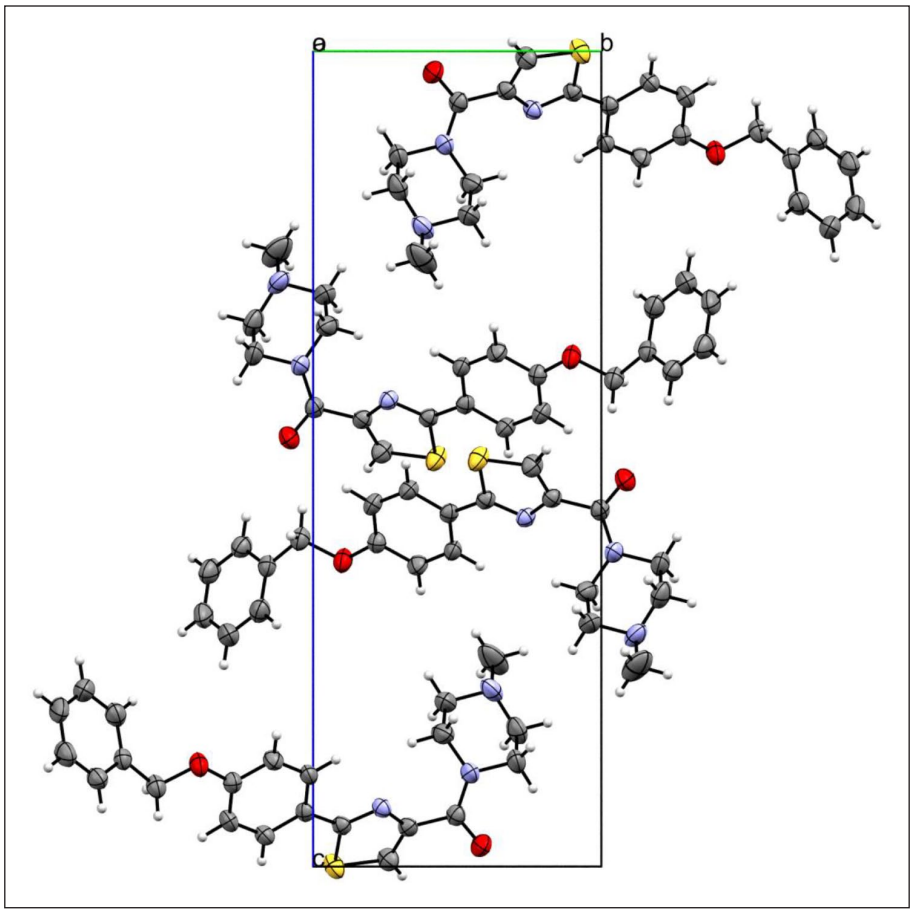

Figure 4. Packing diagram of compound **6a** viewed along the a-axis.

6d were 1.342 and 1.312 Å. The packing diagrams of compounds **6a** and **6d** viewed along the a-axis are shown in Figures 4 and 6. The crystal packing diagrams of the compounds showed that there were no hydrogen bonds present in the two compounds.

Hirshfeld surface analysis

Hirshfeld surfaces and fingerprint plots of compounds **6a** and **6d** were generated and analyzed in order to understand the different intermolecular interactions and packing modes. The d_{norm} was mapped on the Hirshfeld surface and selected two-dimensional (2D) fingerprint plots of the different interactions in the two compounds are shown in Figure 7. For both compounds **6a** and **6d**, the red regions mainly indicate O···H interactions. The d_{norm} maps of compounds **6a** and **6d** both show one pair of deep-red regions which demonstrate strong C–H···O intermolecular interactions between the thiazole group and the amide group.

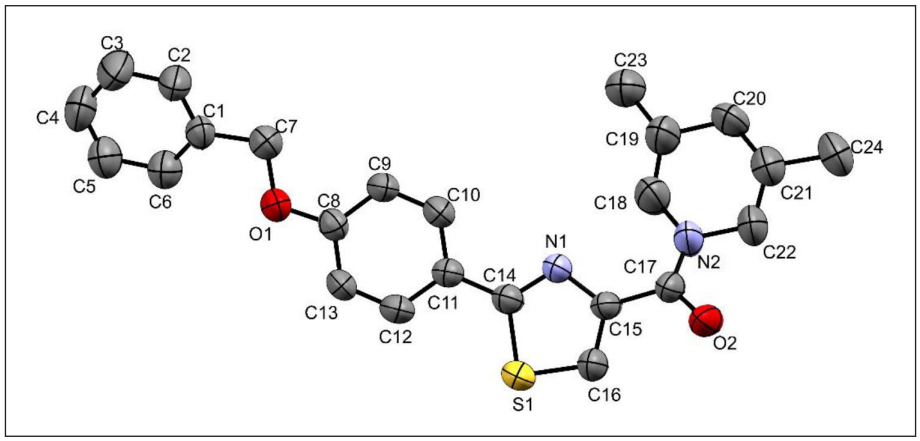

Figure 5. ORTEP representation compound **6d** with thermal ellipsoids drawn at 50% probability.

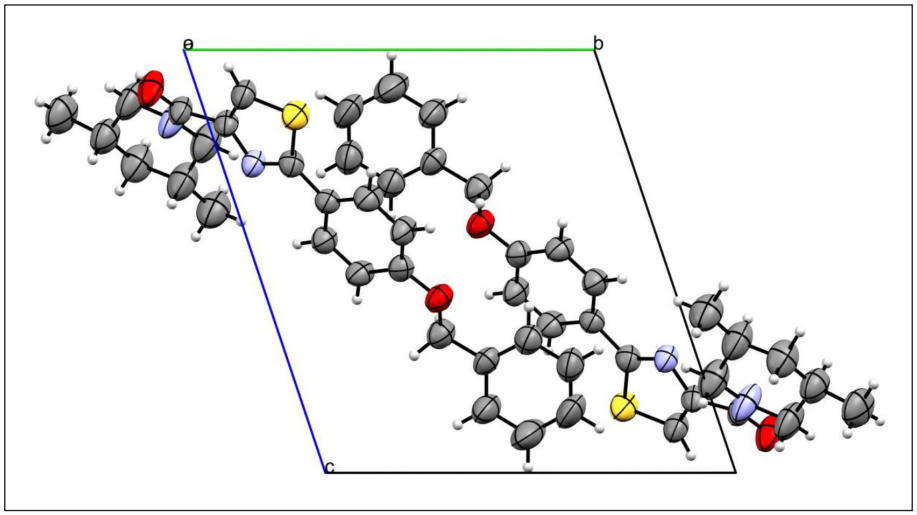

Figure 6. Packing diagram of compound **6d** viewed along the a-axis.

The 2D fingerprint plots of the main intermolecular contacts for compounds **6a** and **6d** are depicted in Figures 8 and 9. H···H intermolecular contacts with contributions of 52.4% and 55.9% of the overall contacts for compounds **6a** and **6d**, respectively, are the major contributors to the Hirshfeld surface. The O···H intermolecular contacts are strong contacts due to the presence of C–H···O intermolecular interactions, contributing to the Hirshfeld surface by 10.2% and 9.2% of the overall contacts for compounds **6a** and **6d**, respectively. Besides the contacts mentioned above, the presence of C···H, N···H, S···H, and other interactions is summarized in Table 3 in the Supplemental material.

In vitro inhibition studies of cholinesterase

The target compounds **6a–d** were studied for their potential as AChE (from *electric eel*) and BuChE (from equine serum) inhibitors using the method described by Ellman et al.[21] In this test, tacrine and donepezil were used as reference drugs and the results of the AChE and BuChE inhibition are presented in Table 1. Among the four derivatives, compound **6d** possessed the best AChEI-inhibitory activity with an IC_{50} value of 8.86 μM and the best BuChE-inhibitory activity with an IC_{50} value of 1.03 μM. A novel series of thiazole acetamide derivatives was reported to possess cholinesterase inhibitory activity. Rahim et al.[17] studied the potential inhibitory activity of 30 thiazole analogues against AChE and BuChE, among which, (*E*)-4-({2-[4-(4-chlorophenyl)thiazol-2-yl]hydrazono} methyl)-benzene-1,2-diol (compound **A**) possessed the best AChE-inhibition activity (IC_{50}=21.3 μM) and best BuChE-inhibition activity (IC_{50}=1.59 μM). 2-(4-Methoxyphenyl)-*N*-(4-phenylthiazol-2-yl)acetamide (compound **B**) showed the best AChE inhibitory activity with an IC_{50} value of 3.14 μM.[16] Compound **6d** (synthesized in this study) showed comparable inhibitory activity toward both enzymes as those of these thiazole derivatives.

Compound **6d** possessed the best BuChE-inhibition activity and inhibited BuChE in a dose-dependent manner (Figure 10). Compounds **6b** and **6c** inhibited BuChE less than 50% at a concentration of 100 μM, implying that the amino substituent on the thiazole derivative played a key role in the cholinesterase inhibition activities of those compounds. Compound **6b** and **6c** showed the good selectivity of AChE with weak BuChE-inhibitory activities at the concentration of 100 μM. Compound **6d** showed poor selectivity of AChE with similar IC_{50} values for AChE and BuChE.

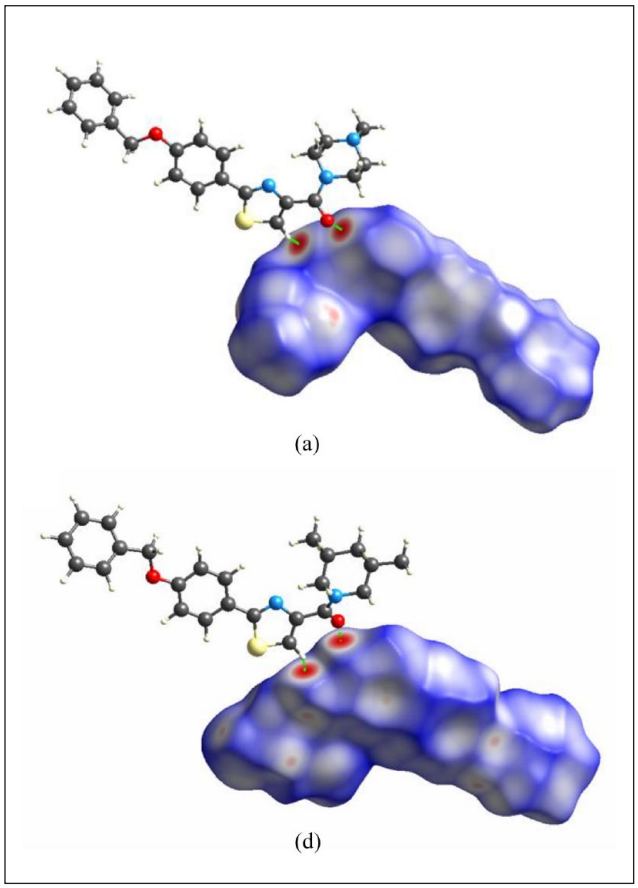

Figure 7. Hirshfeld surfaces mapped with d_{norm} for compounds **6a** and **6d.**

Molecular modeling studies

To understand the binding mode of compound **6d** with AChE and BuChE, it was docked with AChE (PDB code No. 2CMF) and BuChE (PDB code No. 1P0I) using the docking software AUTODOCK4.2 (University of California, San Francisco). The molecular docking of compound **6d** with AChE showed that it could interact with CAS and PAS of AChE (Figure 11). The nitrogen atom of the thiazole group could interact with TYR121 at the PAS site via hydrogen bonds.[22] The benzene ring of the benzyl group can interact with PHE330 and HIS440 (a residue of the catalytic triad in the active site of AChE[23]) via arene–arene interactions. The other benzene ring can interact with PHE288 of the enzyme via an arene–arene interaction. As shown in Figure 12, compound **6d** can interact with the CAS of BuChE. The oxygen atom of the amide group could interact with GLY116 and GLY117 at the CAS site via the hydrogen bonds. The benzene ring on the thiazole group can interact with PHE329 via arene–arene interactions.[24]

Conclusion

In this study, four novel 2-phenylthiazole derivatives were designed, synthesized, and evaluated as cholinesterase inhibitors for the treatment of AD. The structures of the four compounds were determined by IR, NMR, HRMS, and X-ray crystallography. Hirshfeld surface analysis and associated fingerprint plots showed that H···H intermolecular contacts are the major contributor to the Hirshfeld surface. The O···H intermolecular contacts were one of the strong contacts due to the presence of C–H···O intermolecular interactions in compounds **6a** and **6d**. All of the four compounds could inhibit AChE and BuChE. Among them, compound **6d** possessed the best inhibitory activities toward AChE and BuChE. This compound can interact with the PASs of AChE and BuChE and may prove to be a potential lead candidate for the treatment of AD.

Experimental

Materials and methods

All synthetic reagents were purchased from Aladdin Industrial Corporation. All reagents were AR grade and were used without further purification. AChE from electric eel, BuChE from equine serum, 5,5′-dithiobis-(2-nitrobenzoic acid) (DTNB), and butyrylcholine iodide (BTCI) were purchased from Sigma-Aldrich. TLC was performed on glass-backed silica gel sheets (silica gel 60 GF254) and spots were visualized under UV light (254 nm). Melting points were recorded using a Kohler melting point apparatus. ^{1}H NMR and ^{13}C NMR spectra were recorded at 500 MHz using a Bruker Avance III spectrometer. The X-ray single-crystal diffraction data were recorded on a Bruker SMART APEX-II CCD diffractometer. HRMS were performed using an Agilent Technologies 6230 TOF LC/MS instrument.

Synthesis of compounds **6a–d**

The target compounds **6a–d** were synthesized according to Scheme 1. A mixture of *para*-hydroxythiobenzamide (**1**) (3.93 g, 25.67 mmol) and ethyl bromopyruvate (**2**) (5.00 g, 25.64 mmol) in ethanol (50 mL) was refluxed for 4 h. After cooling, distilled water (100 mL) was added. The precipitated solid was filtered and washed with distilled water (50 mL) and dried under reduced pressure to afford ethyl 2-(4-hydroxyphenyl) thiazole-4-carboxylate (**3**) as a white solid.

Yield: 90%. m.p. 78–80 °C. ^{1}H NMR (500 MHz, DMSO-d_6): δ 10.11 (s, 1H), 8.44 (s, 1H), 7.80 (m, 2H), 6.90 (m, 2H), 4.33 (q, J = 7.1 Hz, 2H), 1.33 (t, J = 7.1 Hz, 3H). ^{13}C NMR (126 MHz, DMSO-d_6): δ 168.0, 160.7, 159.9, 146.5, 128.1, 127.7, 123.6, 115.9, 60.6, 14.1.

A mixture of compound **3** (1.00 g, 4.02 mmol) and benzyl bromide (8.04 mmol), K_2CO_3 (1.11 g, 8.04 mmol), and DMF (8 mL) was heated at 80 °C for 8 h, after which the reaction mixture was cooled and distilled water (100 mL) was added. The precipitated solid was filtered and washed with distilled water (50 mL) and dried under reduced pressure to give ethyl 2-(4-benzyloxyphenyl)-thiazole-4-carboxylate (**4**) as a white solid.

Yield: 91%. m.p. 111–113 °C. ^{1}H NMR (500 MHz, $CDCl_3$): δ 8.09 (s, 1H), 8.01–7.90 (m, 2H), 7.50–7.29 (m, 5H), 7.08–6.98 (m, 2H), 5.12 (s, 2H), 4.44 (q, J = 7.1 Hz, 2H), 1.43 (t, J = 7.1 Hz, 3H). ^{13}C NMR (126 MHz, $CDCl_3$):

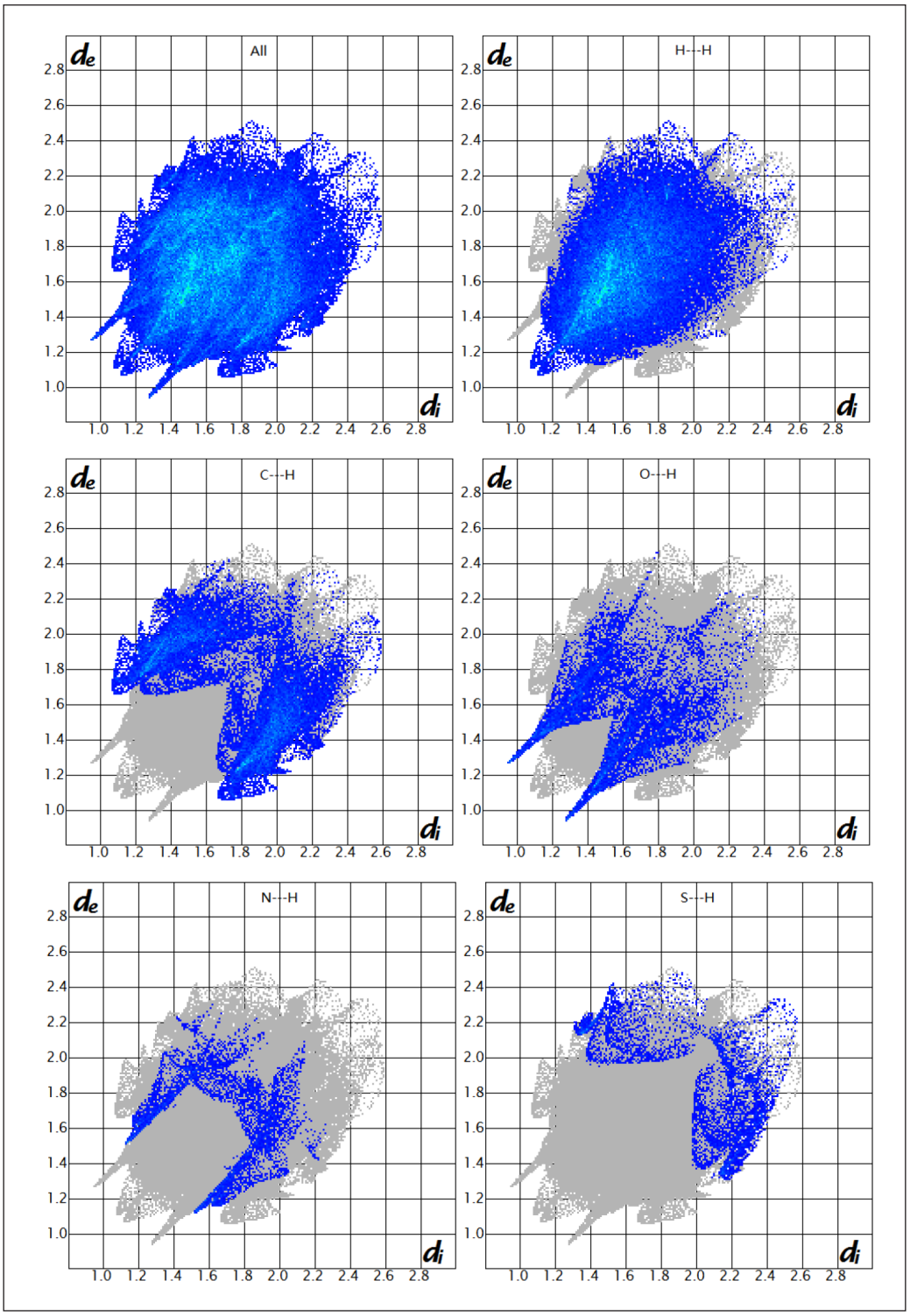

Figure 8. The 2D fingerprint plots of compound **6a**.

δ 168.7, 161.6, 160.8, 147.9, 136.4, 128.5, 128.7, 128.2, 127.5, 126.3, 126.0, 115.2, 70.2, 61.5, 14.4.

Potassium hydroxide (KOH, 0.83 g) was added to a solution of compound **4** (1 g) in anhydrous methanol (15 mL) and the mixture refluxed at 80 °C for 9 h. The solution was then neutralized to pH 5 and poured into cold water (100 mL). The resulting precipitate was filtered and dried to give 2-(4-benzyloxyphenyl)-thiazole-4-carboxylic acid (**5**) as a white solid.

Yield: 89%. m.p. 184–186 °C. ^{1}H NMR (500 MHz, dimethyl sulfoxide (DMSO)-d_6): δ 8.41 (s, 1H), 7.91 (d, J=8.8 Hz, 2H), 7.47 (d, J=7.2 Hz, 2H), 7.41 (t, J=7.4 Hz, 2H), 7.34 (t, J=7.3 Hz, 1H), 7.16 (d, J=8.9 Hz, 2H), 5.19 (s, 2H). ^{13}C NMR (126 MHz, DMSO-d_6): δ 167.7, 162.6, 160.8, 148.4, 137.1, 129.0, 128.5, 128.4, 128.3, 128.2, 126.0, 116.0, 69.94. HRMS (electrospray ionization (ESI)): m/z $[M-H]^-$ calcd for $C_{17}H_{12}NO_3S$: 310.0543; found: 310.0533.

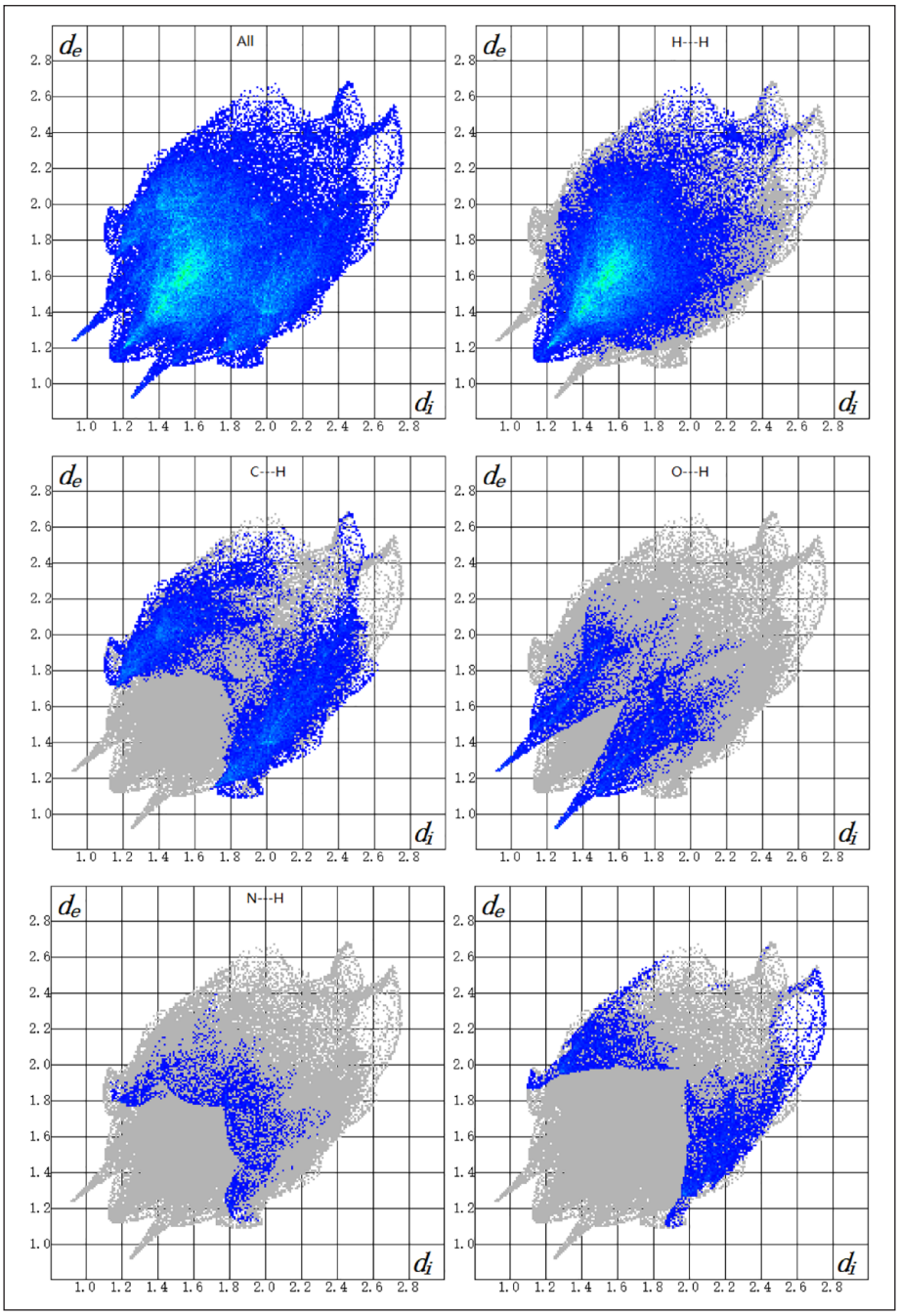

Figure 9. The 2D fingerprint plots of compound **6d**.

Table 1. In vitro inhibition of AChE and BuChE and the selectivity indices of compounds **6a–d.**

Test compound	IC_{50} (μM)		SI[c] (BuChE/AChE)
	AChE[a]	BuChE[b]	
6a	104.03 ± 0.11	71.04 ± 0.16	0.68
6b	39.83 ± 0.11	–	–
6c	66.74 ± 0.08	–	–
6d	8.86 ± 0.08	1.03 ± 0.04	0.116
Donepezil	0.041 ± 0.10	13.10 ± 0.09	318.73
Tacrine	0.18 ± 0.02	0.05 ± 0.01	0.28

[a]50% inhibitory concentration (mean ± standard deviation (SD) of three experiments) of AChE from *electric eel*.
[b]50% inhibitory concentration (mean ± SD of three experiments) of BuChE from equine serum.
[c]Selectivity index for AChE; IC_{50} BuChE/IC_{50} AChE

Thionyl chloride (0.45 mL) was added to a solution of compound **5** (0.4 g) in dichloromethane (10 mL) and the mixture was refluxed at 50 °C for 10 h. When the reaction was complete, the solvent was evaporated under reduced pressure. The residual mass was dissolved in dichloromethane (10 mL) and the corresponding amine (0.23 mL) was added. The solution was refluxed for 6 h. When the reaction was finished, the solvent was evaporated under reduced pressure. The residue was purified using column chromatography (CH_2Cl_2/CH_3OH = 20:1) to give 2-phenylthiazole derivatives **6a–d**. Single crystals of compounds **6a** and **6d** were grown at room temperature from methanol and dichloromethane, respectively.

[2-(4-Benzyloxy-phenyl)-thiazol-4-yl]-(4-methyl-piperazin-1-yl)-methanone (**6a**): Yield: 84%, white solid. m.p. 109–111 °C. IR (KBr): 3079, 1614, 1479, 1249, 1235,

1177, 1011, 1003 cm^{-1}. ^1H NMR (500 MHz, $CDCl_3$): δ 7.88 (d, *J* = 8.9 Hz, 2H), 7.83 (s, 1H), 7.44 (d, *J* = 7.0 Hz, 2H), 7.40 (t, *J* = 7.3 Hz, 2H), 7.35 (t, *J* = 7.2 Hz, 1H), 7.04 (d, *J* = 8.9 Hz, 2H), 5.13 (s, 2H), 4.02 (s, 2H), 3.84 (s, 2H), 2.51 (s, 4H), 2.35 (s, 3H). ^{13}C NMR (126 MHz, $CDCl_3$): δ 167.1, 162.7, 160.6, 151.1, 136.4, 128.7, 128.2, 128.1, 127.5, 126.3, 123.5, 115.3, 70.2, 46.1. HRMS (ESI): *m/z* $[M + H]^+$ calcd for $C_{22}H_{24}N_3O_2S$: 394.1584; found: 394.1620.

2-*(4-Benzyloxy-phenyl)-thiazol-4-carboxylic acid (2-morpholin-4-yl-ethyl)-amide* (**6b**): Yield: 67%, white solid. m.p. 127–129 °C. IR (KBr): 3362, 3127, 2971, 2952, 2885, 2845, 2810, 1669, 1603, 1544, 1486, 1458, 1413, 1249, 1173, 1115, 990 cm^{-1}. ^1H NMR (500 MHz, $CDCl_3$): δ 8.01 (s, 1H), 7.89 (d, *J* = 8.8 Hz, 2H), 7.45 (d, *J* = 7.1 Hz, 2H), 7.41 (t, *J* = 7.4 Hz, 2H), 7.35 (t, *J* = 7.2 Hz, 1H), 7.06 (d, *J* = 8.8 Hz, 2H), 5.14 (s, 2H), 3.83–3.74 (m, 4H), 3.59 (q, *J* = 6.1 Hz, 2H), 2.63 (t, *J* = 6.3 Hz, 2H), 2.55 (s, 4H). ^{13}C NMR (126 MHz, $CDCl_3$): δ 167.9, 161.2, 160.7, 150.7, 136.4, 128.7, 128.2, 128.1, 127.5, 126.1, 121.9, 115.3, 70.2, 67.1, 57.1, 53.3, 35.8. HRMS (ESI): *m/z* $[M + H]^+$ calcd for $C_{23}H_{25}N_3O_3S$: 424.1689; found: 424.1727.

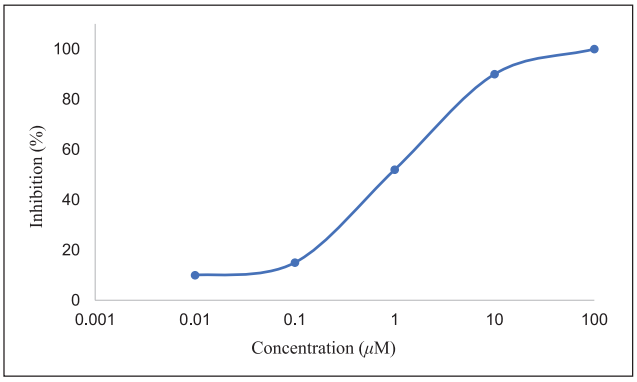

Figure 10. Dose-dependent inhibition of **6d** against BuChE. Values are means ± SD and n = 5.

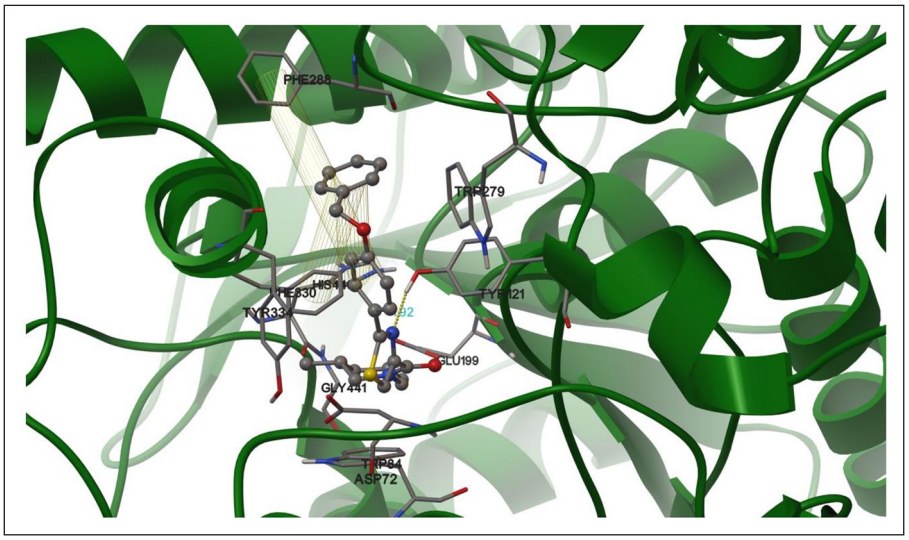

Figure 11. A view of the potential interactions between compound **6d** and the binding site of AChE (PDB No. 2CFM).

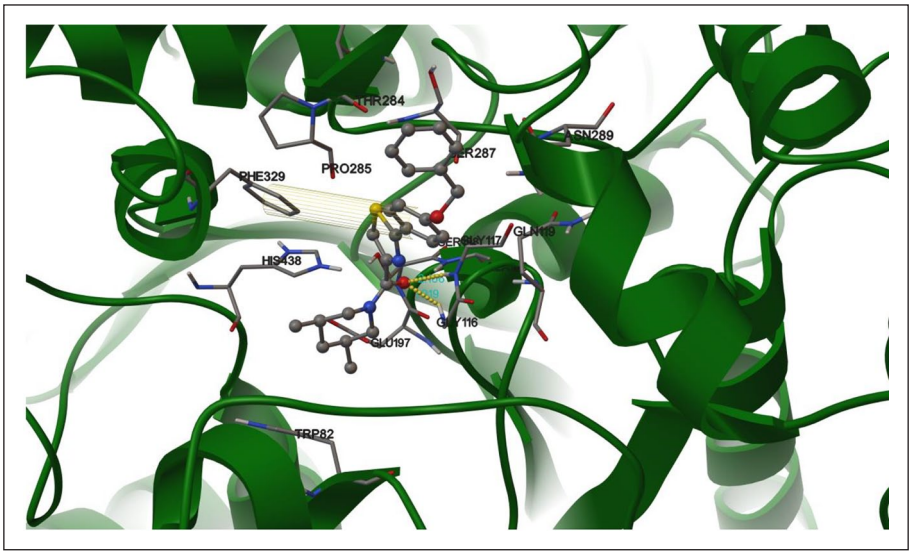

Figure 12. A view of the potential interactions between compound **6d** and the binding site of BuChE (PDB No. 1P0I).

1-*[2-(4-Benzyloxy-phenyl)-thiazol-4-carbonyl]-piperidine-4-carboxylic acid ethyl ester* (**6c**): Yield: 54%, white solid. m.p. 106–108 °C. IR (KBr): 2927, 2860, 1728, 1626, 1607, 1518, 1462, 1251, 1175, 1040, 986 cm^{-1}. ^1H NMR (500 MHz, $CDCl_3$): δ 7.88 (d, *J* = 8.9 Hz, 2H), 7.80 (s, 1H), 7.45 (d, *J* = 7.0 Hz, 2H), 7.40 (t, *J* = 7.4 Hz, 2H), 7.35 (t, *J* = 7.2 Hz, 1H), 7.03 (d, *J* = 8.9 Hz, 2H), 5.13 (s, 2H), 4.54 (d, *J* = 13.3 Hz, 2H), 4.17 (q, *J* = 7.1 Hz, 2H), 3.38–3.24 (m, 1H), 3.12–2.99 (m, 1H), 2.64–2.59 (m, 1H), 2.12–1.93 (m, 2H), 1.92–1.77 (m, 2H), 1.27 (t, *J* = 7.1 Hz, 3H). ^{13}C NMR (126 MHz, $CDCl_3$): δ 174.3, 167.0, 162.9, 160.6, 151.2, 136.4, 128.7, 128.2, 128.1, 127.5, 126.3, 123.1, 115.3, 70.2, 60.6, 41.2, 14.2. HRMS (ESI): *m/z* $[M + H]^+$ calcd for $C_{25}H_{27}N_2O_4S$: 451.1686; found: 451.1726.

[2-(4-benzyloxy-phenyl)-thiazol-4-yl]-(3,5-dimethyl-piperidin-1-yl)-methanone (**6d**): Mixture of cis and trans. Yield: 80%, white solid. m.p. 96–98 °C. IR (KBr): 3088, 2954, 2921, 1605, 1460, 1250, 1227, 1172 cm^{-1}. ^1H NMR (500 MHz, $CDCl_3$): δ 7.88 (d, *J* = 8.8 Hz, 2H), 7.75 (s, 1H), 7.44 (d, *J* = 7.1 Hz, 2H), 7.40 (t, *J* = 7.4 Hz, 2H), 7.34 (t, *J* = 7.2 Hz, 1H), 7.03 (d, *J* = 8.8 Hz, 2H), 5.13 (s, 2H), 4.69 (d, *J* = 12.1 Hz, 1H), 4.48 (d, *J* = 12.8 Hz, 1H), 2.56 (t, *J* = 12.2 Hz, 1H), 2.23 (t, *J* = 12.0 Hz, 1H), 1.88 (d, *J* = 12.9 Hz, 1H), 1.78 (s, 1H), 1.65 (s, 1H), 1.25 (q, *J* = 6.5 Hz, 1H), 0.96 (d, *J* = 6.4 Hz, 3H), 0.88 (d, *J* = 5.8 Hz, 3H). ^{13}C NMR (126 MHz, $CDCl_3$): δ 166.9, 162.6, 160.5, 151.6, 136.4, 128.7, 128.2, 128.1, 127.5, 126.4, 122.5, 115.3, 70.1, 54.4, 49.9, 42.6, 32.3, 31.2, 19.2, 19.0. HRMS (ESI): *m/z* $[M + H]^+$ calcd for $C_{24}H_{27}N_2O_2S$: 407.1788; found: 407.1827.

Single-crystal XRD studies

Crystals of compounds **6a** and **6d** was grown by slow evaporation from methanol and dichloromethane at room temperature, respectively. Diffraction intensities for the compounds were collected at 296(2) K using a Bruker SMART APEX-II CCD area-detector with Mo*K*α radiation (λ = 0.71073 Å). The collected data were reduced with the SAINT program,[25] and multi-scan absorption corrections were performed using the SADABS program.[26] Structures were solved by direct methods. The compounds were refined against F^2 by full-matrix least-squares methods using Olex2.[27] All the non-hydrogen atoms were refined anisotropically. Hydrogen atoms were placed in calculated positions and constrained to ride on their parent atoms. The Mercury program[28] was used to describe the molecular structures. The crystallographic data for the compounds are summarized in Table 1. Crystallographic data for the compounds have been deposited with the Cambridge Crystallographic Data Center [CCDC 2023105 (**6a**) and CCDC 2023106 (**6d**)].

Declaration of conflicting interests

The author(s) declared no potential conflicts of interest with respect to the research, authorship, and/or publication of this paper.

Funding

The author(s) disclosed receipt of the following financial support for the research, authorship, and/or publication of this article: The authors acknowledge the financial support from the Natural Science Foundation of Jiangsu Province (No. BK20191470), the National Natural Science Foundation of China (No. 81703557), and a project funded by the Priority Academic Program Development of Jiangsu Higher Education Institutions.

ORCID iD

Da-Hua Shi https://orcid.org/0000-0002-3101-0418

Supplemental material

Supplemental material for this paper is available online.

References

1. Goedert M and Spillantini MG. *Science* 2006; 314: 777.
2. Goedert M and Ghetti B. *Brain Pathol* 2007; 17: 57.
3. Masters CL, Bateman R, Blennow K, et al. *Nat Rev Dis Primers* 2015; 1: 15056.
4. Wagstaff A and McTavish D. *Drugs Aging* 1994; 4: 510.
5. Burns A, Rossor M, Hecker J, et al. *Dement Geriatr Cogn Disord* 1998; 10: 237.
6. Birks J and Harvey R. *Cochrane Database Syst Rev* 2006; 1: CD001190.
7. Scott L and Goa K. *Drugs* 2000; 60: 1095.
8. Desai A and Grossberg G. *Expert Rev Neurother* 2005; 5: 563.
9. Lan J-S, Ding Y, Liu Y, et al. *Eur J Med Chem* 2017; 139.
10. Li Q, Yang H, Chen Y, et al. *Eur J Med Chem* 2017; 132: 294.
11. Montanari S, Scalvini L, Bartolini M, et al. *J Med Chem* 2016; 59.
12. Siddiqui N, Ahuja P, Ahsan W, et al. *J Chem Pharm Res* 2009; 1.
13. Mishra CB, Kumari S and Tiwari M. *Eur J Med Chem* 2015; 92: 1.
14. Xu Y, Jian MM, Han C, et al. *Bioorg Med Chem Lett* 2020; 30: 126985.
15. Turan-Zitouni G, Altıntop MD, Özdemir A, et al. *Eur J Med Chem* 2016; 107: 288.
16. Sun Z-Q, Tu L-X, Zhuo F-J, et al. *Bioorg Med Chem Lett* 2016; 26: 747.
17. Rahim F, Javed MT, Ullah H, et al. *Bioorg Chem* 2015; 62: 106.
18. Anand P, Singh B and Singh N. *Bioorg Med Chem* 2012; 20: 1175.
19. Ghotbi G, Mahdavi M, Najafi Z, et al. *Bioorg Chem* 2020; 103: 104186.
20. Shi DH, Ma XD, Tang ZM, et al. *J Mol Struct* 2018; 1173: 81.
21. Ellman GL, Courtney KD, Andres V Jr, et al. *Biochem Pharmacol* 1961; 7: 88.
22. Aljohani G, Ali AA-S, Said MA, et al. *J Mol Struct* 2020; 1222.
23. Sussman JC and Harel M. *Science* 1991; 253: 872.
24. Nicolet Y, Lockridge O, Masson P, et al. *J Biol Chem* 2003; 278: 41141.
25. Bruker. *SMART (Version 5628) and SAINT (Version 602)*. Madison, WI: Bruker AXS Inc., 1998.
26. Sheldrick GM. *SADABS program for empirical absorption correction of area detector*. Gottingen: University of Gottingen, 1996.
27. Dolomanov OV, Bourhis LJ, Gildea RJ, et al. *J Appl Crystallogr* 2009; 42: 339.
28. Macrae CF, Bruno IJ, Chisholm JA, et al. *J Appl Crystallogr* 2008; 41: 466.